AIAA 98-2621

An Aerodynamic Assessment of Micro-Drag Generators (MDGs)

Steven X. S. Bauer
NASA Langley Research Center
Hampton, Virginia

16th AIAA Applied Aerodynamics Conference
June 15-18, 1998 / Albuquerque, NM

An Aerodynamic Assessment of Micro-Drag Generators (MDGs)

Steven X. S. Bauer*
NASA Langley Research Center
Hampton, Virginia

ABSTRACT

Commercial transports as well as fighter aircraft of the future are being designed with very low drag (friction and pressure). Concurrently, commuter airports are being built or envisioned to be built in the centers of metropolitan areas where shorter runways and/or reduced noise footprints on takeoff and landing are required. These requirements and the fact that drag is lower on new vehicles than on older aircraft have resulted in vehicles that require a large amount of braking force (from landing-gear brakes, spoilers, high-lift flaps, thrust reversers, etc.). Micro-drag generators (MDGs) were envisioned to create a uniformly distributed drag force along a vehicle by forcing the flow to separate on the aft-facing surface of a series of deployable devices, thus, generating drag. The devices are intended to work at any speed and for any type of vehicle (aircraft, ground vehicles, sea-faring vehicles). MDGs were applied to a general aviation wing and a representative fuselage shape and tested in two subsonic wind tunnels. The results showed increases in drag of 2 to 6 times that of a "clean" configuration.

INTRODUCTION

Today's aircraft are designed with ever decreasing values of drag to improve fuel economy, increase range, and increase payloads. With decreasing vehicle drag, it is becoming more and more important to consider methods of deceleration. In addition, both military and commercial aircraft require lightweight, efficient control surfaces. Since 1988, the NASA Langley Research Center has been investigating advanced aircraft control effectors. This research has focused on developing flow management concepts and control concepts that satisfy multidisciplinary design issues for military aircraft. Micro-Drag Generators (MDGs, Ref. 1) were one of the concepts developed under these programs. In addition to aerodynamic control effectiveness, MDGs were found to be quite effective at braking and aerodynamic deceleration for all vehicles.

*Aerospace Engineer, Configuration Aerodynamics Branch, Member AIAA

It is the objective of this paper to introduce a unique flow management concept that can be applied to any class of vehicle to change the drag. The concept uses small deployable devices referred to as MDGs that individually generate small amounts of drag, but when deployed in large numbers can generate substantial amounts of drag. The micro-drag generators (MDGs) may be thought of as miniature spoilers or speed brakes. During normal operation of the vehicle (e.g., during cruise), the devices would not be extended into the flowfield and would not increase the drag of the vehicle. When actuated, the MDGs work in the same manner as stall strips. They are designed to force the flow on a vehicle to separate on the aft-facing side of the device and when spaced correctly, to allow the flow to reattach before reaching the next device. This allows substantial amounts of drag to be generated with a simple system of small (micro) devices. The drag generated by a system of MDGs is expected to be equivalent to that which would be expected from a single device with the same projected area as the sum of all the MDG projected areas. The benefits of having a number of small devices instead of one large device are: reduction in weight of actuators, increase in safety because several MDGs could fail without a large effect on drag generation capability compared to a failure of a single component braking system, and a uniform distribution of load (i.e., drag) which is of particular importance for tractor-trailer rigs on ice or rain covered roads.

Aircraft decelerate by deflecting flaps and spoilers, wheel brakes, and thrust reversers. Ground vehicles (e.g., automobiles, tractor-trailers, buses, trains, etc.) are also designed for low drag. In this case, deceleration is accomplished by using disc or drum brakes. Oil tankers, aircraft carriers, and other large ships typically reverse directions on their screws to decelerate or coast (for a mile or more) until their momentum is reduced to the point that a tugboat can take over and pilot the ship to a pier.

In addition to deceleration, MDGs could be used as a control effector, if applied asymmetrically to a vehicle (i.e., applied to one wing or one side of the fuselage and not the other). Because these devices are small (and thus, do not protrude "far" into the flowfield), they are also attractive for military aircraft survivability. In addition, these MDGs may be used to provide drag for braking of ground vehicles (e.g., cars, trucks, buses, trains, etc.) and ships (e.g., sailboats, motorboats, barges, transports, submarines, etc.). The application of the device to tractor-trailers would allow such vehicles the capability of improved braking on ice or rain covered surfaces and since the device can be applied to the trailer, the braking would not cause the vehicle to "jack-knife" as may occur with conventional braking systems.

This paper will discuss how MDGs work and present data on drag increases found on wind-tunnel models tested at NASA Langley Research Center test facilities.

NOMENCLATURE

b	wing span, inches
c	chord, inches
C_D	drag coefficient, $\frac{\text{Drag}}{q_\infty S}$
C_L	lift coefficient, $\frac{\text{Lift}}{q_\infty S}$
$C_{L,max}$	maximum value of C_L
C_l	rolling-moment coefficient, $\frac{\text{Rolling moment}}{q_\infty Sb}$
C_n	yawing-moment coefficient, $\frac{\text{Yawing moment}}{q_\infty Sb}$
D_{RS}/D_{SR}	Ratio of the Drag of a Ridge System to Drag of a Single Ridge
h	height of MDG, inches
L	characteristic length (chord), inches
M_∞	Freestream Mach number
N	number of MDGs
q_∞	Freestream dynamic pressure, psf
s	ridge spacing, inches
S	Reference Area, ft^2
t	width of MDG (or ridge), inches
x	distance in the streamwise direction, inches
α	angle of attack, degrees
Δ	Change in force or moment

MDG Designation

XDYZ Designation Format

X MDG Density [L (Low), M (Medium), H (High)]

D Density

Y Size [S (Small), L (Large)]

Z Type [B (Hemispherical Bumps), P (Vertical Drag Plates)]

Examples

- LDSB Low Density, Small Hemispherical Bumps
- MDSB Medium Density, Small Hemispherical Bumps
- HDSB High Density, Small Hemispherical Bumps
- LDLB Low Density, Large Hemispherical Bumps
- MDLB Medium Density, Large Hemispherical Bumps
- HDLB High Density, Large Hemispherical Bumps
- LDSP Low Density, Small Vertical Plates
- MDSP Medium Density, Small Vertical Plates
- HDSP High Density, Small Vertical Plates
- LDLP Low Density, Large Vertical Plates
- MDLP Medium Density, Large Vertical Plates
- HDLP High Density, Large Vertical Plates

DESCRIPTION OF WIND TUNNELS AND MODELS

Wind Tunnel Facilities

A General Aviation (Whitcomb) number one [GA(W)-1] wing model was tested in the NASA Langley Research Center, 14- by 22-Foot Subsonic Wind Tunnel which is a closed-circuit, single-return, atmospheric wind tunnel with a test section that can be operated in a variety of configurations – closed, slotted, partially open, and open (Reference 2). The closed section configuration is 14.5 ft high by 21.75 ft wide by 50 ft long with a maximum speed of about

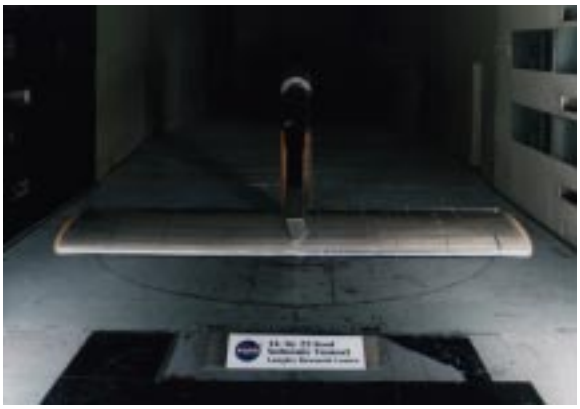

Figure 1. GA(W)-1 model installed in the NASA LaRC 14- by 22-Foot Subsonic tunnel.

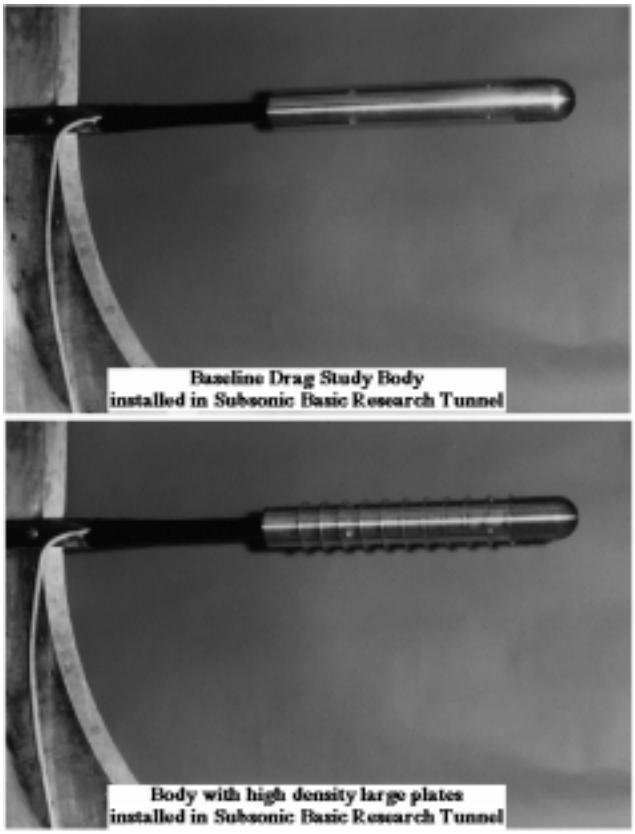

Figure 2. Drag Body Configurations D1 (baseline) and D7.2 Installed in NASA LaRC SBRT.

338 ft/sec. The tests run on the GA(W)-1 model were conducted at dynamic pressures, q_∞, of 45 and 60 psf (0.17 to 0.20 Mach). Figure 1 shows the GA(W)-1 model installed in the 14- by 22-Foot test section.

In addition to the GA(W)-1 test, hemispherical-capped, cylindrical drag bodies were tested in the NASA Langley Research Center, Subsonic Basic Research Tunnel (SBRT). SBRT is a low speed facility with a 24- by 24-inch test section. The tunnel operates at dynamic pressures, q_∞, from 7 to 40 psf. Figure 2 shows two of the test models installed in the NASA LaRC SBRT facility.

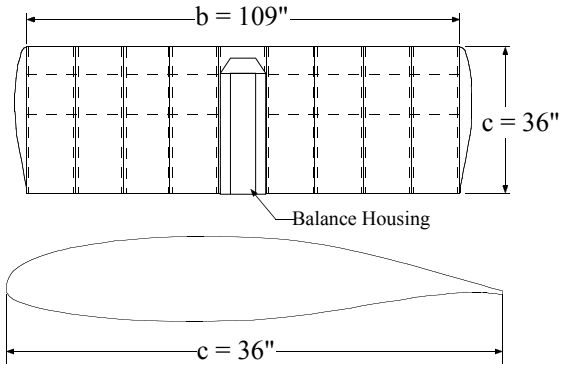

Figure 3. GA(W)-1 airfoil and schematic of wing planform.

Wind Tunnel Models

The present experimental investigations of the MDG concept utilized hemispherical bumps and vertical plates applied to a wing and a series of representative fuselage shapes. However, the MDG concept is applicable to rectangular, triangular, or any other shape of protuberance.

The GA(W)-1 wind tunnel model is shown in schematic form in figure 3. The wing had a 0°-swept planform incorporating a GA(W)-1 airfoil. The GA(W)-1 is a general airfoil section developed to provide performance increases over conventional airfoils at subcritical conditions. The airfoil is 17 percent thick with a fairly blunt leading edge and a cusped lower surface, trailing edge. The design C_L is 0.4 and the wing was designed to have good lift-to-drag ratios at C_L of 1.0 (for climb); $C_{L,max}$ occurs near a C_L of 2.0. In addition, the airfoil has a blunt trailing edge with nearly equal upper and lower surface slopes to moderate the pressure recovery on the upper surface and postpone trailing edge separation and stall (References 3 and 4). The model had a 109-inch span and a 36-inch chord. The center panel had a balance housing, and forces/moments were recorded using a 6-component strain gauge balance.

Figures 4 and 5 show photographs of the GA(W)-1 airfoil model with various MDG systems installed on the surface. Figures 4a-c show the wing

Figure 4a. GA(W)-1 model with Large Vertical Plates and high density distribution (HDLP).

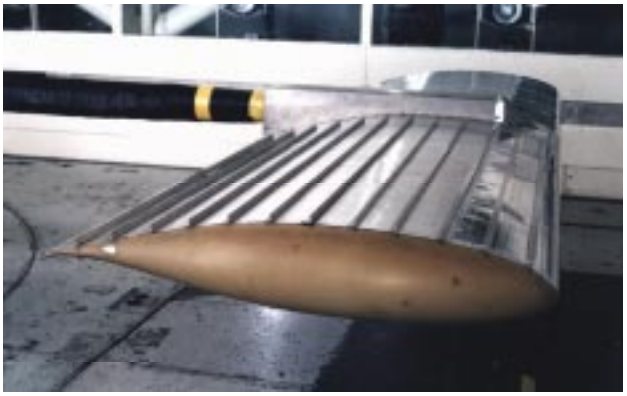

Figure 4b. GA(W)-1 model with Large Vertical Plates and medium density distribution (MDLP).

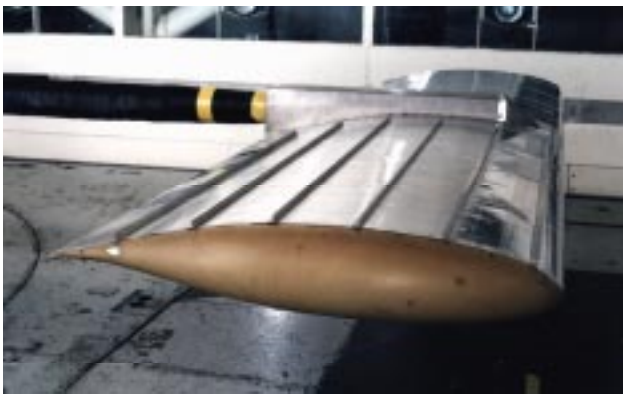

Figure 4c. GA(W)-1 model with Large Vertical Plates and low density distribution (LDLP).

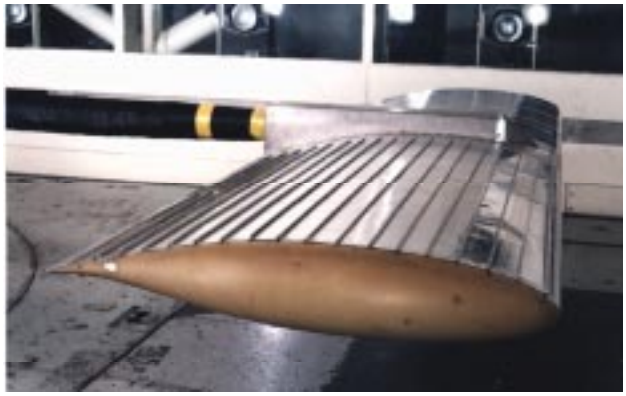

Figure 5a. GA(W)-1 model with Small Vertical Plates and high density distribution (HDSP).

Figure 5b. GA(W)-1 model with Large Hemispherical Bumps and high density distribution (HDLB).

Figure 5c. GA(W)-1 model with Small Hemispherical Bumps and high density distribution (HDSB).

with high, medium, and low density, large vertical plates (h=1/2 in.). Figures 5a-c show the wing with the high density, small plates (1/4 in.), large hemispherical bumps (1/2 in.), and small hemispherical bumps (1/4 in.).

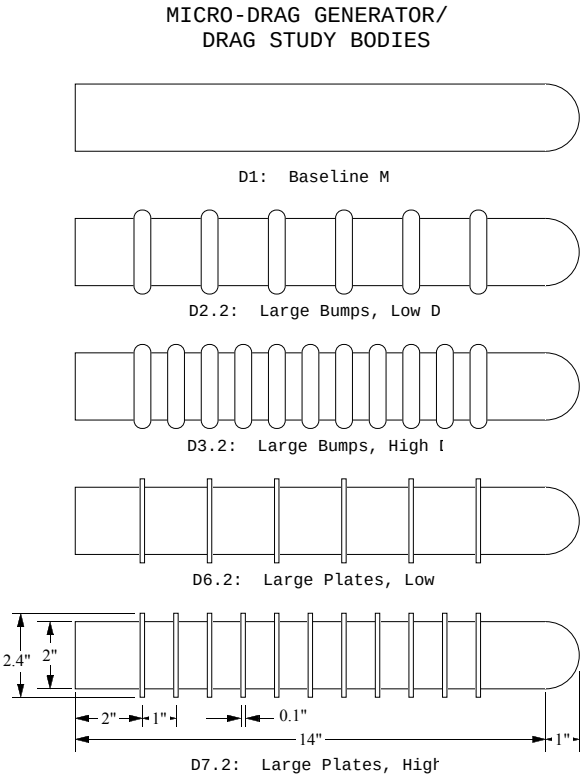

Figure 6. Hemispherical - Capped, Cylindrical Drag Bodies.

It should be pointed out that the size of the plates and bumps has been enlarged to match the size of the boundary layers that would occur in the wind tunnel. Flight hardware would require smaller MDGs than the scaled-up versions of the wind-tunnel models.

Twelve, 14-inch long Micro-Drag Generator/dragbodies were fabricatedand tested in the NASA LaRC SBRT facility. Sketches of the baseline and four of the drag bodies tested in the SBRT facility are shown in figure 6. Variations in MDG shape and spacing were investigated to determinethe "best" method of generating drag on an aircraft fuselage or for application on a ground vehicle.

RESULTS AND DISCUSSION

Background

The MDG concept takes advantage of flow separation characteristics over surface protuberances oriented approximately perpendicular to the local flow direction. The MDGs would be deployed when required (through the surface of the vehicle; utilizing a variety of actuation concepts such as microactuation, Shape Memory Alloy (SMA) actuation or blown up [like a balloon], to extend the required amount into the flowfield). It should be noted that non-actuating "stall strips" have been used on aircraft for many years to prematurely stall the flow (to cause separation to occur in a more predictable manner) usually on the upper surface of the wing. Figure 7 illustrates the flow separation and reattachment behind a hemispherical ridge and a vertical plate or rectangular ridge. The flow downstream of these shapes is very similar in size and strength, thus producing similar drag increases and lift losses. Reference 5 describes the separation characteristics of different shapes and how the separation varies with boundary layer thickness; references 6 through 10 describe how to estimate excrescence drag due to various protuberances on flight hardware.

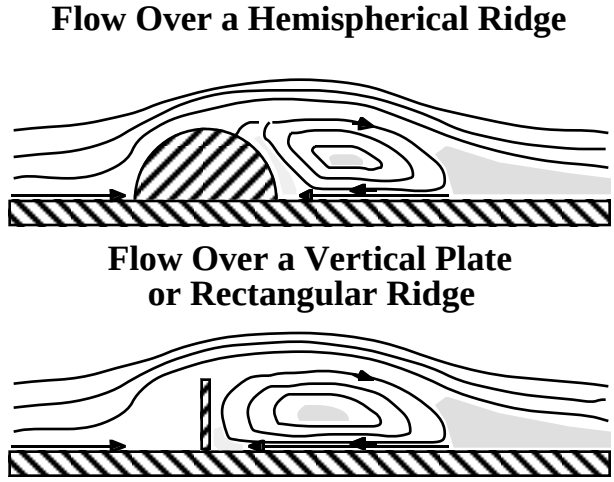

Figure 7. Schematic of Flow Separation over a hemispherical bump and a vertical plate.

Reference 11 describes how drag varies for different profile shapes of ridges (i.e., non-actuating MDGs) placed on flat plates. The author also discusses how the height and width affect the drag of an individual ridge as well as rules for spacing of

ridges to optimize drag generation. These rules will be discussed in the next few paragraphs.

Flow Over a Series of Hemispherical Ridges

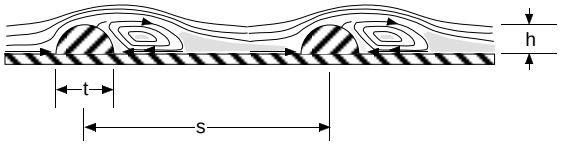

Figure 8. Schematic of Flow Separation over multiple MDGs.

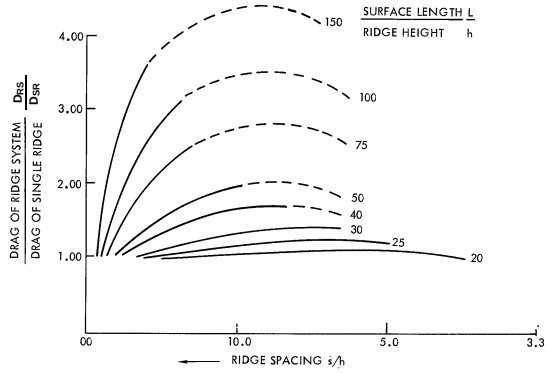

Figure 9. Variation in drag due to height of ridge and spacing between ridges for a zero pressure gradient.

Figure 8 illustrates the parameters available for producing optimum drag generation. When the spacing between ridges is too large, the number of ridges, N, will be low and the resulting drag generation will be low. When the spacing between the ridges is too small, the drag will again be low, because the separation from the previous ridge will interfere with the downstream ridge effectiveness (burying the downstream ridge in the wake of the upstream ridge and thus, reducing the effective height of the downstream ridge). Figure 9 (from reference 11) is a plot of the ratio of the drag of the total ridge system to the drag of a single ridge (D_{RS}/D_{SR}) versus ridge spacing to height ratio (s/h). Plotted are curves of constant surface length to ridge height (L/h). The plot indicates that a system of small ridges or MDGs can be more effective than one MDG. The optimum drag generation potential is then a function of the shape, the size, and the spacing of the MDGs. Figure 9 and references 5 through 11 were used extensively in the design of the wind-tunnel hardware.

Discussion of Wind-Tunnel Results

In reference 5, it was determined from wind-tunnel tests that when properly spaced, the larger the bump, the higher the drag. Thus, by properly spacing the distance between MDGs of a given height, the flow separates downstream of the MDG and reattaches just upstream of the next MDG. It was found that the drag was greater for MDG shapes that had a flat face normal to the flowfield (i.e., plates) than for rounded shapes. The results obtained on MDGs and for all the data presented in this paper are for low speeds ($M_\infty \leq 0.20$) and for low Reynolds numbers.

Table 1 describes the Configuration number, MDG profile (e.g., low density small bumps-LDSB), number of MDGs (N), and size as applied to the GA(W)-1 wing. The table also points out which configurations were asymmetric (MDGs applied only to one side of the wing, i.e., the left-hand side [LHS]).

Table 1: Description of MDG Configurations tested on the GA(W)-1 Model.

Config.	MDG Profile	Number of MDGs	Size, h (inches)
400	LDSB	6	0.25
401	MDSB	12	0.25
402	HDSB	18	0.25
403	LDLB	6	0.50
404	MDLB	12	0.50
405	HDLB	18	0.50
406	LDSP	6	0.25
407	MDSP	12	0.25
408	HDSP	18	0.25
412	MDSB	12 (LHS)	0.25
413	MDLB	12 (LHS)	0.50
414	MDSP	12(LHS)	0.25
415	LDLP	6	0.50
416	MDLP	12	0.50
417	MDLP	12 (LHS)	0.50

Figure 10a illustrates how spacing affects the lift and drag characteristics of the GA(W)-1 wing with 0.25-inch hemispherical drag bumps and figure 10b compares spacing effects with 0.25-inch drag plates. The MDGs were placed on both the upper and lower surfaces of the wing in order to take

maximum advantage of the surface area on which to increase the drag.

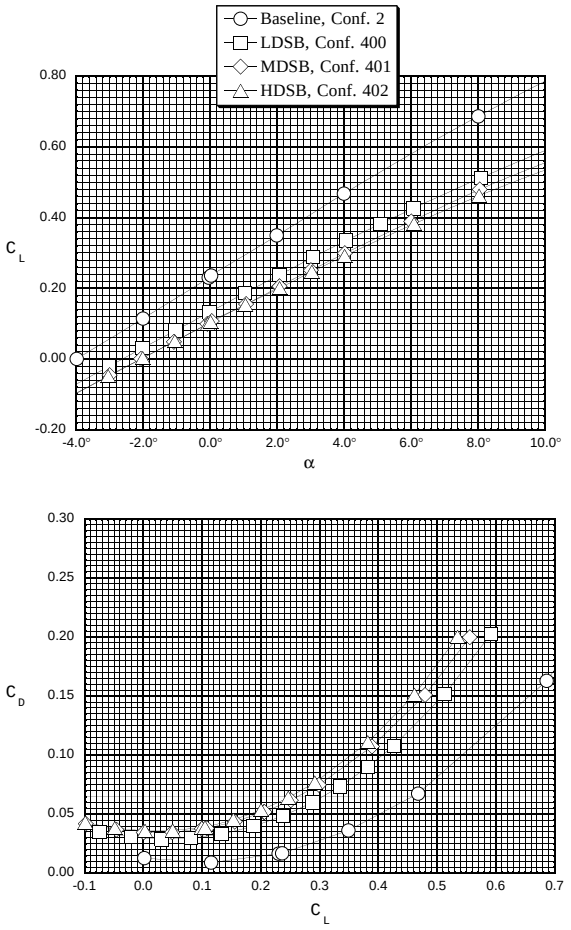

Figure 10a. Lift and drag characteristics of the GA(W)-1 wing effect of small drag bumps ($M_\infty = 0.20$).

In figure 10a, the lift is reduced for any application of MDGs on the surface. This occurs because most of the wing upper and lower surfaces have separated flow occurring on them. Even though the wing appears thicker to the flow (because of the layer of separation on the upper and lower surfaces) the flow is unable to expand to the same levels on the upper surface leading edge (as was evident in surface pressure data, not included in this report). Thus, the reduction in pressure difference between the upper and lower surfaces reduces the lift. The drag also increases for each of the MDG configurations tested with the largest increase in drag occurring for the highest density system. However, the difference in drag generation between the medium and the high density distributions is not very great. Figure 10b shows very similar results for the small plate configurations. By referring back to figure 9, an optimum spacing may be achieved with fewer MDGs; therefore, a minimum spacing between MDGs may have been reached with a configuration that falls between the medium density and high density configurations. Due to system complexity and weight, the medium density may provide the optimum spacing and will be investigated further in the following figures.

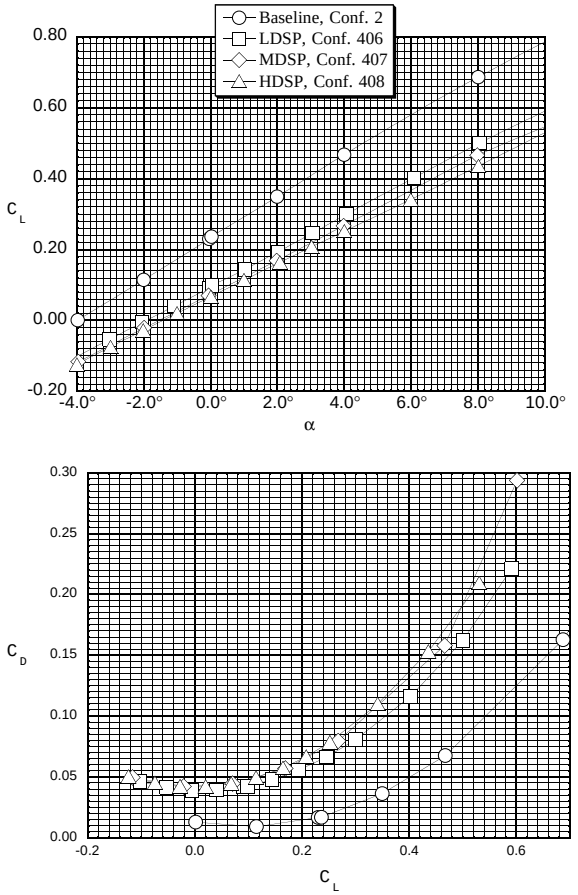

Figure 10b. Lift and drag characteristics of the GA(W)-1 wing effect of small drag plates ($M_\infty = 0.20$).

Figure 11 shows the difference in drag generation between 0.25 inch and 0.50 inch plates and hemispherical bumps with medium density spacing. Even though the drag is highest for the drag plates, drag levels on the rounded bumps is nearly as high and has characteristics that may be more appealing to military aircraft mission survivability and may be more easily applied by use of SMA technology.

Figure 12 shows the change in lift and drag (subtracting the baseline lift coefficient value at the same angle of attack and baseline drag coefficient

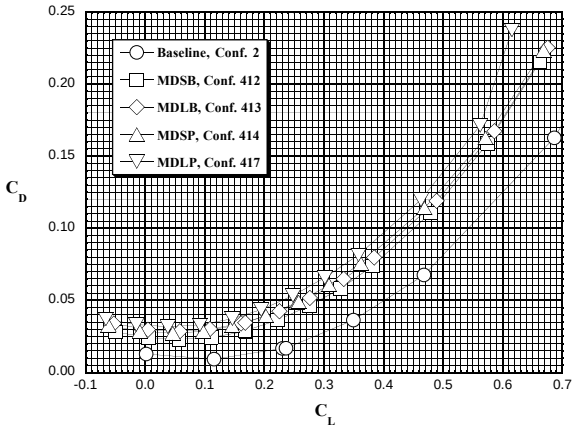

Figure 11. Drag characteristics of the GA(W)-1 wing effect of small drag plates (M_∞ = 0.20, Medium Density spacing).

value at the same lift coefficient) and the percent difference in drag for the four configurations plotted in figure 11. For all four configurations, the change in lift is always negative and decreases linearly with angle of attack and the change in drag is always positive and increases with increasing lift. The percent increase in drag due to MDG application clearly shows that the hemispherical bumps generate as much as 340% and 460% more drag than the baseline for the MDSB and MDLB configurations, respectively. The increase in drag for the plate MDGs is as much as 460% and 570% for the MDSP and MDLP configurations, respectively. Figure 12 clearly indicates that plates are more effective at generating drag and reducing lift; however, hemispherical MDGs also generate sizable changes in lift and drag and may be more acceptable for certain applications and configurations.

Since MDGs reduce the lift, deployment of MDGs on one side of the aircraft (i.e., one wing or one side of the fuselage) is expected to generate a rolling moment. Since drag is also generated when MDGs are deployed, an accompanying yawing-moment coefficient would also be expected. The control effectiveness (capability to generate an asymmetric force or moment) resulting from deployment of MDGs on the left-hand side (LHS) of the wing only is clearly shown in figure 13. As indicated in figure 13a, the baseline wing had non-zero yawing-moment coefficients (due primarily to geometrical asymmetries in the balance housing at the centerline of the GAW-1 model shown in figure 1). When MDGs were applied to the surface, substantial moment coefficient values (C_n and C_l)

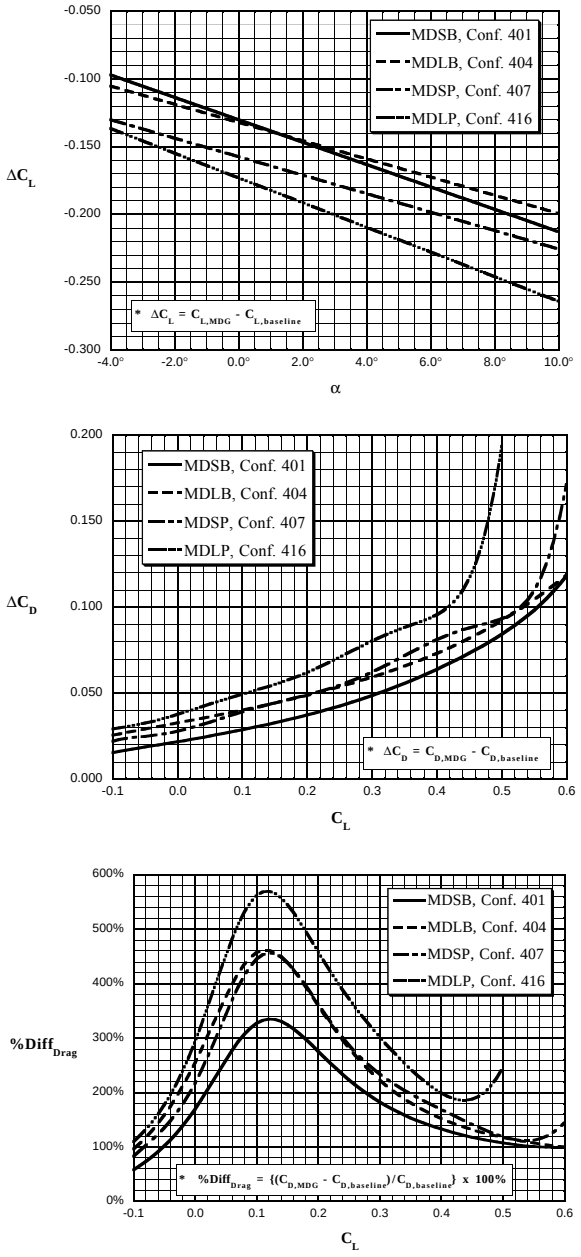

Figure 12. Change in lift and drag coefficient values as well as the percent difference in drag due to bumps or plates (M_∞ = 0.20).

were generated (figure 13a). The changes in ΔC_n and ΔC_l (figure 13b) suggest the potential for MDGs as control effectors. MDG control effectors could be used to augment existing control surfaces (thus, reducing the size and weight of existing devices) or used alone (eliminating existing devices). The plots also show that this type of control effector has

substantial control authority even at low lift conditions. Some control effectors generate large

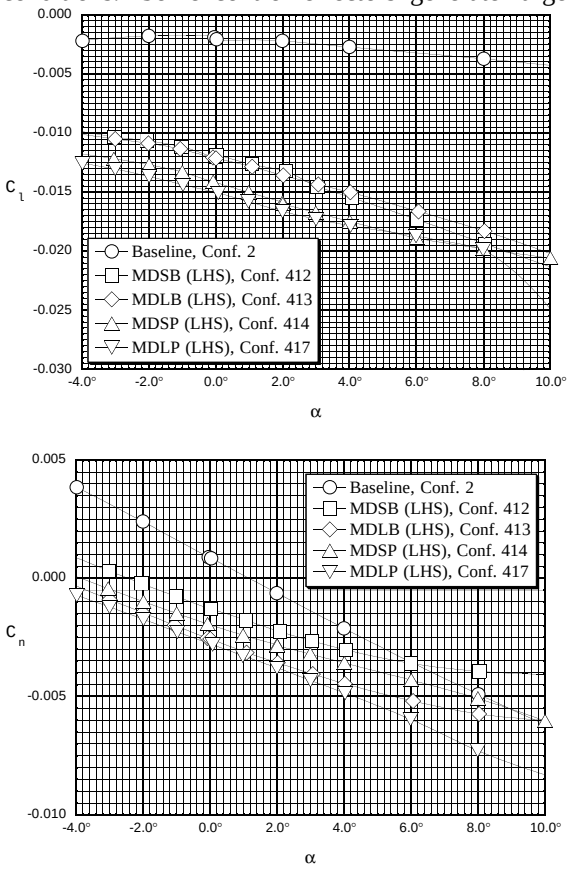

Figure 13a. The rolling- and yawing-moment characteristics of the GA(W)-1 wing with MDGs installed on left-hand-side (LHS) of wing ($M_\infty = 0.20$).

moments at low angles of attack and others at high angles of attack; MDGs appear to generate substantial moments across the angle of attack range (i.e., for all lift conditions).

The second part of this experimental program was to explore MDGs for non-lifting surfaces such as fuselages or ground vehicles. The next few figures will discuss experimental results for MDG applications on hemispherical-capped, cylindrical bodies tested over a range of dynamic pressures at 0° angle of attack.

Figure 14 presents the effect of dynamic pressure on two of the cylindrical drag bodies (i.e., the baseline D1 and the HDLP D7.2 configuration). These results indicate that the drag increment resulting from MDG deployment on the D7.2 configurations (see figure 6) remained nearly constant with increasing dynamic pressure. Drag coefficient values varied from 0.3 to 0.4 on the baseline (D1)

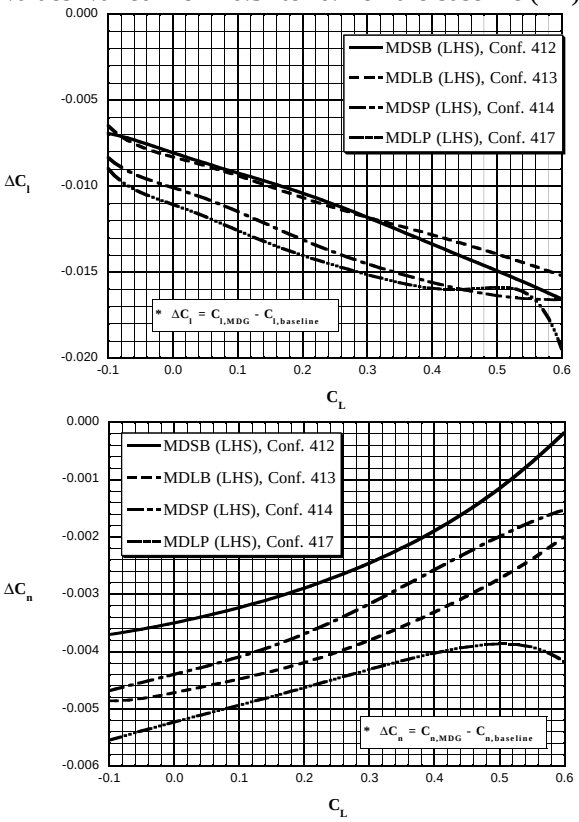

Figure 13b. The change in rolling- and yawing-moment characteristics of the GA(W)-1 wing with MDGs installed on left-hand-side (LHS) of wing ($M_\infty = 0.20$).

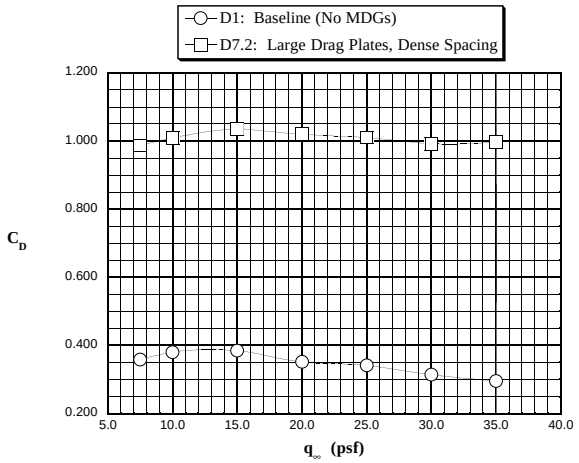

Figure 14. Drag Coefficient versus dynamic pressure for the baseline drag body and Configuration D7.2 (Large Plates, High Density HDLP) drag body ($\alpha = 0.0°$)

configuration and were approximately 1.0 to 1.05 for the large, densely-spaced drag plate (D7.2)

configuration. This implies that, if properly placed on a configuration, an increase in drag on a fuselage (or applied to a tractor trailer) of 2.5 to 3.0 could be expected. The level of increase in drag for the MDGs on the cylindrical drag bodies was fairly constant across the speed range. The velocities tested were from 55 mph to 117 mph. These velocities are consistent with general aviation and transport aircraft landing speeds and with speeds for ground vehicles on highways.

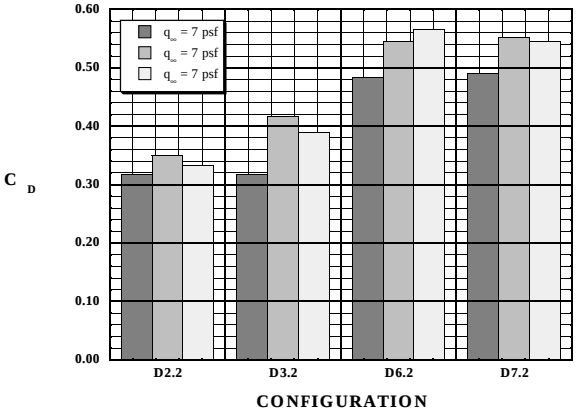

Figure 15. Comparison of Drag Bodies at three dynamic pressures.

Figure 15 presents the change in drag for a given drag body as compared to the baseline configurations for three different dynamic pressures. Overall the drag plate configurations (D6.2 and D7.2) produced more drag than the drag bump configurations (D2.2 and D3.2). For ground vehicles, the drag plates would probably be the easier of the two concepts discussed in this paper to implement (either as sliding plates that would be inserted vertically normal to the body surface or as slats that could be deflected up much like a venetian blind). For aircraft applications, the hemispherical bumps or plates utilizing SMAs may be most cost effective.

CONCLUDING REMARKS

Micro-Drag Generators (MDGs) have been found to be very effective at generating drag in the speed range tested. By at least doubling the drag on the fuselage and wing, an aircraft would be able to stop much more quickly and with less wear on landing-gear braking systems, and without as much reliance on conventional spoilers, high-lift devices, and thrust reversers. On ground vehicles, the added safety of having the MDGs applied to trailers on tractor-trailer rigs might greatly reducethe number of accidents caused by "jack-knifing" on wet or icy roadways. Because MDGs are very nonintrusive, the application of such devices on military aircraft as a control effector is quite attractive (reduced weight and complexity over conventional devices especially if SMAs could be implemented in the design of the devices).

The wind-tunnel data showed that the deployment of MDGs on a wing can increase the drag by as much as 570% and on a fuselage a 350% increase is attainable. It was found that more, large devices produced higher drag values than a few, small devices. Plates were generally found to outperform hemispherical bumps. Also, substantial amounts of control effectiveness (both rolling- and yawing-moment coefficients) could be generated by asymmetrically applying MDGs to an aircraft. Therefore, MDGs appear to be an effective device for decelerating or controlling a vehicle. Because of the redundancy (numerous actuated surfaces) and because of the uniform force generated, these devices appear to be a safe alternative to existing systems.

Application of MDGs to transonic and supersonic vehicles has been proposed and will be investigated in the future. Maturation of MDGs for aerodynamic control at flight Reynolds numbers and at transonic and supersonic speeds is also being considered. Finally, application of MDGs to ground vehicles is already underway and application to aircraft, watercraft, and other vehicles will require the development of smart, lightweight materials to efficiently incorporate MDGs.

REFERENCES

1. Bauer, S. X. S. and Wood, R. M.: Micro-Drag Generators for Aerobraking and Control. NASA Patent Application LAR 15245-1, 1994.

2. Gentry, G. L., Jr.; Quinto, P. F.; Gatlin, G. M.; and Applin, Z. T.: The Langley 14- by 22-Foot Subsonic Tunnel: Description, Flow Characteristics, and Guide for Users. NASA TP-3008. September 1990.

3. McGhee, R. J. and Beasley, W. D.: Low-Speed Aerodynamic Characteristics of a 17-Percent –Thick Airfoil Section Designed for General Aviation Applications. NASA TN D-7428. December 1973.

4. Ayers, T. G.: Supercritical Aerodynamics: Worthwhile Over a Range of Speeds. Astronautics & Aeronautics, vol. 10, no. 8, pages 32-36, August 1972.

5. Hoerner, Dr. S. F.: Fluid-Dynamic Drag, Published by the Author, 1965.

6. Gaudet, L. and Johnson, P.: Measurements of the Drag of Various Two-Dimensional Excrescences Immersed in Turbulent Boundary Layers at Mach Numbers between 0.2 and 1.8. RAE TR 70190, 1970.

7. Gaudet, L. and Winter, K. G.: Measurements of the Drag of Some Characteristic Aircraft Excrescences Immersed in Turbulent Boundary Layers. AGARD CP No. 124, Aerodynamic Drag, Paper 4. 1973.

8. Good, M. C. and Joubert, P. N.: The Form Drag of Two-Dimensional Bluff Bodies Immersed in Turbulent Boundary Layers. J.F.M. 31, Pt. 3., pages 547-582. 1968.

9. Jones, R. C. and Williams, D. H.: The Effects of Surface Roughness on Characteristics of Aerofoils NACA 0012 and RAF 34, ARC R&M No. 1708. 1936.

10. Nash, J. F. and Bradshaw, P.: The Magnification of Roughness Drag by Pressure Gradients. J.R.Ae.S. 71, pages 44-49. 1967.

11. Young, A. D. and Paterson, J. H.: Aircraft Excrescence Drag. AGARD-AG-264. 1981.